Variable Entangling in a Quantum Battle of the Sexes Cellular Automaton

Ramón Alonso-Sanz

Technical University of Madrid, ETSIA (Estadística, GSC)
C.Universitaria, Madrid 28040, Spain
ramon.alonso@upm.es

Abstract. The effect of variable entangling on the dynamics of a spatial quantum formulation of the iterated battle of the sexes game is studied in this work. The game is played in the cellular automata manner, i.e., with local and synchronous interaction. The effect of spatial structure is assessed when allowing the players to adopt quantum and classical strategies, both in the two and three parameter strategy spaces.

1 Introduction

1.1 The Classic Context

The so-called *battle of the sexes* (BOS) is a simple example of a two-person (♀ and ♂) asymmetric game, i.e., a game whose payoff matrices are not coincident after transposition. Thus, $\mathbf{P}_{♂} = \begin{pmatrix} R & 0 \\ 0 & r \end{pmatrix}$, and $\mathbf{P}_{♀} = \begin{pmatrix} r & 0 \\ 0 & R \end{pmatrix}$. The rewards $R > r > 0$ quantify the preferences in a conventional couple fitting the traditional stereotypes: the male prefers to attend a *F*ootball match, whereas the female prefers to attend a *B*allet performance. Both players hope to *coordinate* their choices, but the *conflict* is also present because their preferred activities differ [14].

Using uncorrelated probabilistic strategies $\mathbf{x} = (x, 1-x)'$ and $\mathbf{y} = (y, 1-y)'$, the expected payoffs (p) in the BOS game are:

$$p_{♂}(x;y) = \mathbf{x}'\mathbf{P}_{♂}\mathbf{y} \quad , \quad p_{♀}(y;x) = \mathbf{x}'\mathbf{P}_{♀}\mathbf{y}\,. \tag{1}$$

The pair of strategies $(\mathbf{x}, \mathbf{y})$ are in Nash equilibrium if $\mathbf{x}$ is a best response to $\mathbf{y}$ and $\mathbf{y}$ is a best response to $\mathbf{x}$. The three pairs of strategies in Nash equilibrium in the BOS game are: $x = y = 0$, $x = y = 1$, and $\big(x = R/(R+r), y = 1-x\big)$. Both players get the same payoff if $y = 1-x$, with a maximum $p^+ = (R+r)/4$ for $x = y = 1/2$.

In a different game scenario, the players have not an active role, instead of it a probability distribution $\mathbf{\Pi} = (\pi_{ij})$ assigns probability to every combination of player choices, so $\mathbf{\Pi} = \begin{pmatrix} \pi_{11} & \pi_{12} \\ \pi_{21} & \pi_{22} \end{pmatrix}$ in 2×2 games [14]. Thus, the expected payoffs

J. Was, G.C. Sirakoulis, and S. Bandini (Eds.): ACRI 2014, LNCS 8751, pp. 125–135, 2014.

in the BOS are: $\begin{matrix} p_{\male} = \pi_{11}R + \pi_{22}r \\ p_{\female} = \pi_{11}r + \pi_{22}R \end{matrix}$. If $\pi_{11} = \pi_{22} = \pi$, both players get the same payoff $p^{=} = \pi(R + r)$, which if $\pi > 1/4$ is not accessible in the uncorrelated strategies scenario; with maximum $p^{+} = (R + r)/2$ if $\pi = 1/2$.

The quantum approach described in the next subsection, participates of both the independent active players model (1), and the so-called correlated games, where an *external* random device $\mathbf{\Pi}$ determines the players moves.

1.2 Quantum Games

In the quantization scheme introduced by Eisert et al. [8], the classical pure strategies are assigned two basic vectors $|0\rangle$ and $|1\rangle$ respectively, in a Hilbert space of a two level system. The state of the game is a vector in the tensor product space spanned by the basis vectors $|00\rangle$, $|01\rangle$, $|10\rangle$, $|11\rangle$, where the first and second entries in the ket refer to the players A and B respectively.

The quantum game protocol starts with an initial entangled state $|\psi_i\rangle = \hat{J}|00\rangle$, where $\hat{J}$ is a symmetric unitary operator that *entangles* the player's qubits and that is known to both players. To ensure that the classical game is a subset of its quantum version, it is necessary that $\hat{J} = exp(i\frac{\gamma}{2}\hat{D}^{\otimes 2})$, where $\gamma \in [0, \pi/2]$. Thus,

$$\hat{J}|00\rangle = \begin{pmatrix} \cos(\gamma/2) & 0 & 0 & i\sin(\gamma/2) \\ 0 & \cos(\gamma/2) & -i\sin(\gamma/2) & 0 \\ 0 & -i\sin(\gamma/2) & \cos(\gamma/2) & 0 \\ i\sin(\gamma/2) & 0 & 0 & \cos(\gamma/2) \end{pmatrix} \begin{pmatrix} 1 \\ 0 \\ 0 \\ 0 \end{pmatrix} = \begin{pmatrix} \cos(\gamma/2) \\ 0 \\ 0 \\ i\sin(\gamma/2) \end{pmatrix}.$$

The players choose independently their quantum strategies as local unitary operators ($\hat{U}$), $\hat{U}_A$ and $\hat{U}_B$. After the application of these strategies, the state of the game evolves to $|\psi_{f_o}\rangle = (\hat{U}_A \otimes \hat{U}_B)\hat{J}|00\rangle$. Prior to measurement, the $\hat{J}^{\dagger}$ gate is applied and the state of the game becomes:

$$|\psi_f\rangle = \hat{J}^{\dagger}(\hat{U}_A \otimes \hat{U}_B)\hat{J}|00\rangle \equiv (\psi_1\ \psi_2\ \psi_3\ \psi_4)' \tag{2}$$

This follows a pair of Stern-Gerlach type detectors for measurement. As a result, $\mathbf{\Pi} = \begin{pmatrix} |\psi_1|^2\ |\psi_2|^2 \\ |\psi_3|^2\ |\psi_4|^2 \end{pmatrix}$. Consequently, the expected payoffs in the BOS become:

$$p_{\begin{Bmatrix} \male \\ \female \end{Bmatrix}} = \begin{Bmatrix} R \\ r \end{Bmatrix} |\psi_1|^2 + \begin{Bmatrix} r \\ R \end{Bmatrix} |\psi_4|^2 \tag{3}$$

We will considerer here the two-parameter subset of the SU(2) space of strategies:

$$\hat{U}(\theta, \alpha) = \begin{pmatrix} e^{i\alpha}\cos(\theta/2) & \sin(\theta/2) \\ -\sin(\theta/2) & e^{-i\alpha}\cos(\theta/2) \end{pmatrix}, \begin{matrix} \theta \in [0, \pi] \\ \alpha \in [0, \pi/2] \end{matrix}. \tag{4}$$

If $\alpha_A{=}\alpha_B = 0$, or if $\gamma = 0$, it turns out (denoting $\omega \equiv \theta/2$):

$$\mathbf{\Pi}=\begin{pmatrix}\cos^2\omega_A\cos^2\omega_B & \cos^2\omega_A\sin^2\omega_B\\ \sin^2\omega_A\cos^2\omega_B & \sin^2\omega_A\sin^2\omega_B\end{pmatrix}=\begin{pmatrix}\cos^2\omega_A\\ \sin^2\omega_A\end{pmatrix}\left(\cos^2\omega_B\ \sin^2\omega_B\right)\ . \quad (5)$$

Thus, the joint probabilities factorize as in the *classical* game employing independent strategies (1) with $x=\cos^2\omega_A$, $y=\cos^2\omega_B$. So to say, the θ parameters are the *classical* ones. In the classic $\gamma=0$ context, exactly middle-levels of the θ and α parameters lead to $\mathbf{\Pi}=\begin{pmatrix}1/4 & 1/4\\ 1/4 & 1/4\end{pmatrix}$. Thus, in the BOS game: $p_{\male}=p_{\female}=(R+r)/4$.

In contrast, with maximal entangling ($\gamma=\pi/2$), if θ_A=θ_B=0, it is: $\mathbf{\Pi}=\begin{pmatrix}\cos^2(\alpha_A+\alpha_B) & 0\\ 0 & \sin^2(\alpha_A+\alpha_B)\end{pmatrix}$, a non-factorizable probability distribution. With $\gamma=\pi/2$ and equal middle-level election of the parameters by both players, $\mathbf{\Pi}$ degenerates, as $\pi_{22}=1$. Thus, the two-parameter strategies model (4) is somehow biased towards the female player.

We will consider here also the three-parameter strategies [5] scenario:

$$\hat{U}(\theta,\alpha,\beta)=\begin{pmatrix}e^{i\alpha}\cos(\theta/2) & e^{i\beta}\sin(\theta/2)\\ -e^{-i\beta}\sin(\theta/2) & e^{-i\alpha}\cos(\theta/2)\end{pmatrix}\ ,\ \begin{matrix}\theta\in[0,\pi]\\ \alpha,\beta\in[0,\pi/2]\end{matrix}\ . \quad (6)$$

2 The Spatialized QBOS

In the spatial version of the BOS we deal with, each player occupies a site (i,j) in a two-dimensional $N\times N$ lattice. We will consider that *males* and *females* alternate in the site occupation. Thus, both kind of players are arranged in a chessboard form, so that every player is surrounded by four partners (♀-♂, ♂-♀), and four mates (♀-♀, ♂-♂).

In a cellular automata (CA)-like implementation, in each generation (T) every player plays with his four adjacent partners, so that the payoff $p_{i,j}^{(T)}$ of a given individual is the sum over these four interactions. In the next generation, every player will adopt the parameter choice $(\alpha_{i,j}^{(T)},\theta_{i,j}^{(T)})$ of his nearest-neighbor mate (including himself) that received the highest payoff. In case of a tie, the player maintains his choice.

Details of the *male-female* site occupation, as well as simple examples of the initial dynamics, are given in [2,3]. Incidentally, an initial study of the spatialized quantum prisoner's dilemma was reported in [1].

All the simulations in this work are run in a $N=200$ lattice with periodic boundary conditions and initial random assignment of the parameter values. Thus, initially: $\overline{\theta}\simeq\pi/2=1.57$, and $\overline{\alpha}\simeq\pi/4=0.78$. The computations have been performed by a double precision Fortran code run on a mainframe.

Figure 1 shows the long-term ($T=200$) mean payoffs across the lattice ($\overline{p}$) in five simulations of a two-parameter quantum (5,1)-BOS CA with variable entanglement factor γ. The bias towards the female player in the model with maximal entangling (pointed out in the Introduction section) becomes apparent

in Fig. 1 for high γ values, specifically for $\gamma > 3\pi/8$. In contrast to this, the initial increase of the entangling factor, from the classic $\gamma = 0$ context, leads to a dramatic bifurcation of the mean payoffs in favor to the male player, reaching a peak close to (5,1) when γ approaches $\pi/8$. Before, but close, this value of γ, both mean payoffs commence a smooth approach as γ increases, reaching fairly equal values by $\gamma \simeq 3\pi/8$.

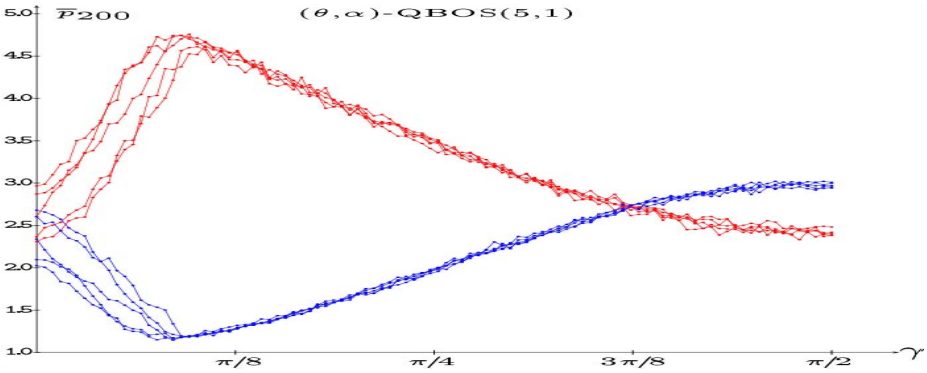

Fig. 1. Long-term mean payoffs in five simulations of a two-parameter quantum (5,1)-BOS CA with entangling factor γ

Figure 2 shows how the main features of the plots in Fig. 1 remain with the (2,1), (4,1) and (6,1) BOS parameters, though in the $R = 2$ case with a fairly flat appearance, and in the $R = 4$ case with the region with low γ rather noisy.

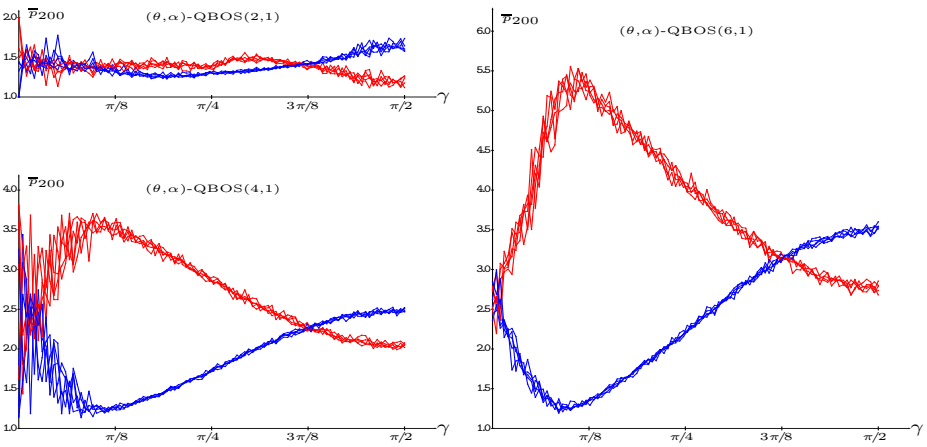

Fig. 2. Long-term mean payoffs in five simulations of two-parameter quantum (2,1), (4,1) and (6,1)-BOS CA with entangling factor γ

Examples of the dynamics and long-term patterns in the scenario of Fig. 1 for particular fairly high γ values may be found in [3]. A further example in shown here in Fig.3, which deals with a very low entanglement factor: $\gamma = \pi/16$. The far left panel of the figure shows the evolution up to T=200 of the mean values across the lattice of θ, α as well of the actual ($\overline{\mathbf{p}}$) and theoretical mean payoffs. The $\overline{\theta}$ values evolve initially in opposite direction from their mean values, close to $\pi/2 = 1.57$, $\overline{\theta}_{\male}$ decreases up to 0.699, whereas $\overline{\theta}_{\female}$ grows up to 2.411. But the ulterior dynamics depletes this high $\overline{\theta}_{\female}$ value, so that it fairly stabilizes it in a low value, and $T = 200$ it is $\overline{\theta}_{\female} = 0.654$. The $\overline{\theta}_{\male}$ parameter decreases up to 0.364 at $T = 200$. The dynamics of both $\overline{\alpha}$ parameter values is smoother compared to that of $\overline{\theta}$, so from the initial $\overline{\alpha} \simeq \pi/4 = 0.78$, at $T = 200$ it is: $\overline{\alpha}_{\male} = 0.794$ and $\overline{\alpha}_{\female} = 0.661$. The parameter dynamics in Fig.3 quickly drives the $\overline{\mathbf{p}}$ mean payoffs to distant values, so that from approximately $T = 10$, the mean female payoff becomes stabilized around $\overline{\mathbf{p}}_{\female} = 1.41$, and from approximately $T = 100$ the male payoff is stabilized around $\overline{\mathbf{p}}_{\male} = 4.12$. Thus, the dynamics clearly favours the process to the male player, a kind of result contrasting with the bias towards the female player in the Eisert et al. model with full entangling.

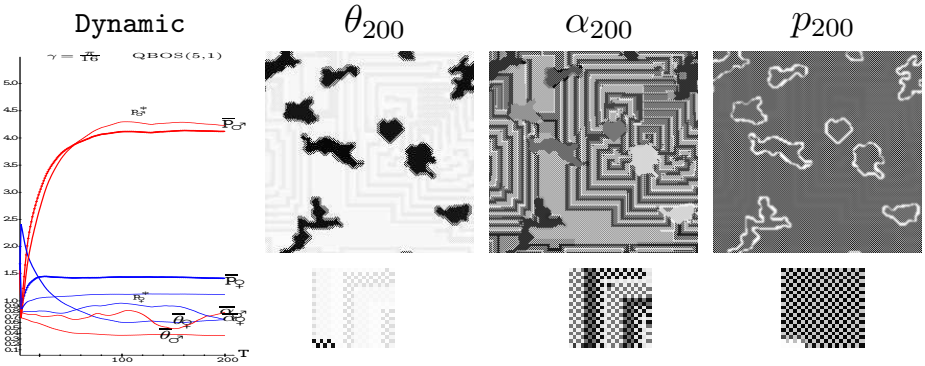

Fig. 3. Simulation of a two-parameter quantum (5,1)-BOS CA with $\gamma = \pi/16$. Far Left: Evolving mean parameters and payoffs. Center: Parameter patterns at T=200. Far Right: Payoff patterns at T=200. Increasing grey levels indicate increasing parameter pattern values.

The curves labelled p^* in the left panel of Fig. 3 show the *theoretical* (or *mean-field*) payoffs, i.e., the payoffs achieved for both kind of players in a single hypothetical two-person game with players adopting the mean parameters appearing in the spatial dynamic simulation. Namely,

$$U^*_{\male} = \begin{pmatrix} e^{i\overline{\alpha}_{\male}} \cos\overline{\omega}_{\male} & \sin\overline{\omega}_{\male} \\ \sin\overline{\omega}_{\male} & e^{-i\overline{\alpha}_{\male}} \cos\overline{\omega}_{\male} \end{pmatrix} \quad , \quad U^*_{\female} = \begin{pmatrix} e^{i\overline{\alpha}_{\female}} \cos\overline{\omega}_{\female} & \sin\overline{\omega}_{\female} \\ \sin\overline{\omega}_{\female} & e^{-i\overline{\alpha}_{\female}} \cos\overline{\omega}_{\female} \end{pmatrix} .$$

As a general rule, due the spatial heterogeneity in the parameter values, the theoretical mean-field estimations of the mean payoffs are different to the actual ones. In the particular case of Fig. 3 , the theoretical payoffs $\mathbf{p}^*$ estimate fairly well the trends of the actual mean payoffs $\overline{\mathbf{p}}$, but $\mathbf{p}^*_{\male}$ over-estimates $\overline{\mathbf{p}}_{\male}$ and $\mathbf{p}^*_{\female}$ under-estimates $\overline{\mathbf{p}}_{\female}$.

Figure 3 shows also the snapshots of the parameter and payoff patterns at $T = 200$, both for the full lattice and its zoomed 23×23 central part. Both maze-like structures and coordination clusters may be appreciated at some extent in the parameter patterns. In the θ parameter pattern, the maze-like structure is tenuously visible, whereas the coordination clusters stands up. In the α parameter pattern, the maze-like structure is predominant but also coordination clusters are appreciated. Coordination, favouring the male players, predominates in the payoff pattern, where the disagreement becomes apparent in the form of clear (meaning low payoff) closed narrow zones.

For a given value of γ, e.g., $\gamma = \pi/16$ in Fig.3, the variation of the initial parameter pattern configurations only alters minor details of the evolving dynamics, the main features of the dynamics and of the long-term patterns are preserved. As a general rule, as γ increases the maze-like appearance of the parameter patterns in the long-term becomes dominant, and even the payoffs patterns adopt this appearance, as may be seen in [3] for $\gamma = \pi/16$ and for the fully entangled case. As the parameter patterns become fairly only maze-like (with no coordination clusters) as γ increases, the theoretical p^* values tend to poorly reflect the actual mean payoffs of both kinds of players. The spatial structure marks the difference, so that a mean-field approach tends to be less indicative of the actual spatial mean payoffs. A very good example of this may be that of $\gamma = 3\pi/8$, in which case both actual mean payoffs quickly converge to an equal value, whereas their corresponding p^* estimations stand far beyond this common actual value.

Figure 4 shows the long-term mean payoffs in the BOS parameters scenario of Fig. 1, but in the three-parameter strategies model. At variance with what happens in the two parameter scenario (Fig.1), the mean payoffs are not dramatically altered by the variation of γ. The overall effect of the increase of γ being a moderation in the variation of the $\overline{p}$ values that oscillate nearly over 2.5 . Please, note that in the three-parameter strategies model, there is not any bias favoring the female player, so that there is not any tendency to any player over rating the other one. The spatial ordered structure induces a kind of self-organization effect, which allows to achieve fairly soon, approximately at $T = 20$, pairs of mean payoffs that are accessible only with correlated strategies in the two-person game. Recall that the maximum equalitarian payoff in the uncorrelated context is p^+=(R+r)/4=1.5 , whereas the payoffs in the simulations of Fig. 4 with high entanglement factor reach values over 2.5, not far from the maximum feasible equalitarian payoff $p^= = (R + r)/2 = 3.0$.

The main features of the plots in the Fig. 4 have been checked to be preserved with the BOS parameters (2,1) , (4,1) and (6,1) . In these three cases, the general form of the $\overline{\mathbf{p}}$ versus γ plots is that shown here for (5,1) in Fig. 4 , reaching

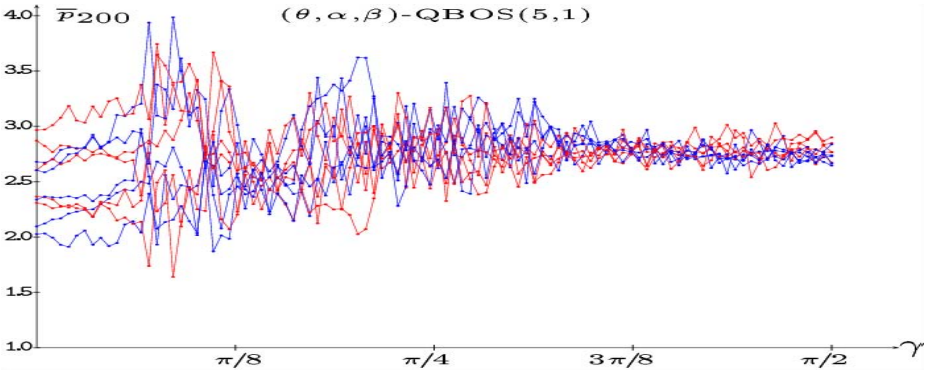

Fig. 4. Long-term mean payoffs in five simulations of a three-parameter quantum (5,1)-BOS CA with entangling factor γ

long-term $\overline{\mathbf{p}}$ values not far from $(R+r)/2$. Thus, with $R=2$ around 1.5, with $R=4$ around 2.25, and with $R=6$ around 3.25.

Examples of the dynamics and long-term patterns in the scenario of Fig. 4 with $\gamma = \pi/2$ may be found in [2]. Early patterns in a particular $\gamma = \pi/2$ simulation are also shown in [2]. Accordingly with the absence of bias favouring any of the types of players, in the three-parameter simulations both mean payoffs, and parameter values evolve in a fairly parallel way. The parameter patterns show a rich structure (enclosing both maze-like and nucleation regions) so that the mean-field estimations $\mathbf{p}^*$ do not follow the actual payoffs $\overline{\mathbf{p}}$.

3 Unfair Contest

Let us assume the unfair situation: A type of players is restricted to classical strategies $\tilde{U}(\theta,0)$, whereas the other type of players may use quantum $\hat{U}(\theta,\alpha)$ ones [9].

Figure 5 shows the long-term mean payoffs in five simulations of an unfair two-parameter quantum male (red) versus classic female (blue) (5,1)-BOS CA with variable entanglement factor γ. The evolution of the mean payoffs of both players is that expected: As soon as γ takes off, the quantum player over rates the classic player. The bifurcation of both $\overline{p}$-values is very rapid, so that by $\pi/4$ the payoff of the classic player is lowered to the stable value 1, whereas that of the quantum player reaches an almost stable value close to 5. With the (4,1) BOS parameters, the plots in the scenario of Fig. 5 do not present a crisp bifurcation-like appearance: They are highly noisy for low γ values, and from nearby $\pi/8$ they change rather abruptly to $p_{\male}$ close to 4, and $p_{\female}$ close to 1. In the same vein, with the (2,1) BOS parameters, the plots are highly noisy, i.e., with no clear advantage for any of the players, up to γ close to $\pi/8$, only beyond this value of the entangling factor, the quantum player over rates the classic one, but in a notable way, e.g., with full entangling: $p_{\male} \simeq 1.5$, $p_{\female} \simeq 1.25$. By contrast, with $(R=6, r=1)$, the bifurcation appearance is more defined than

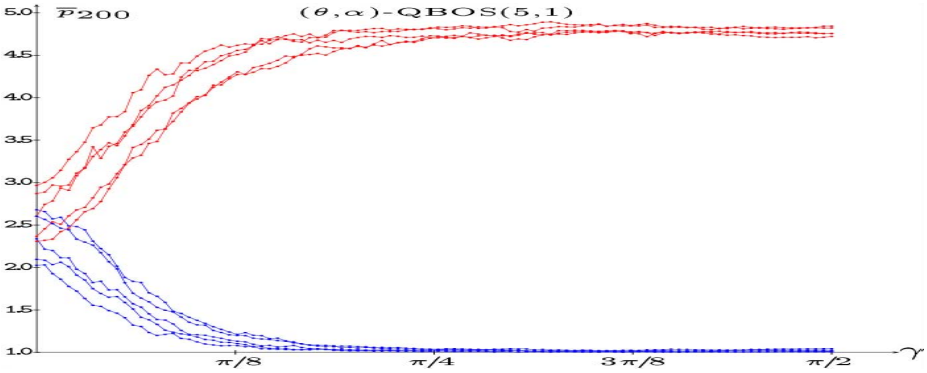

Fig. 5. Long-term mean payoffs in five simulations of an unfair two-parameter quantum (red) versus classic (blue) (5,1)-BOS CA with entanglement factor γ

that shown here for (5,1), with the plots corresponding to the different initial quantum parameter randomizations very close all along their dynamics.

Examples of the dynamics and long-term patterns in the unfair scenario of Fig. 5 with $\gamma = \pi/2$ may be found in [2] . In this scenario, there is a general drift to zero by every parameter, so that the mean-field approach operates properly.

Figure 6 shows the long-term mean payoffs in five simulations of an unfair three-parameter quantum male (red) versus classic female (blue) (5,1)-BOS CA with variable entanglement factor γ . Initially, for low γ, the general appearance of the curves in Fig .6 is the same as that of the Fig .5 . But before $\pi/8$, a kind of phase transition rockets the payoff of the male players and plummets that of the female players. Immediately after this episode, both types of payoffs commence to approach, so that by $\gamma = \pi/4$ they equalize at the level $\overline{p} = 3.0$. After this middle-level of γ , the quantum player increasingly over rates the classic player. With very high levels of γ the monotone evolution of the $\overline{p}$-values appears disrupted, so that the (5,1) payoffs are not reached. Even, coordination fails close to maximal entangling so that the payoff of the classic player goes slightly under $r = 1$ close to $\gamma = \pi/2$. The main features of the plots in Fig. 6 are preserved with the BOS parameters (4,1) and (6,1) ; even the small $\overline{\mathbf{p}}_{\mathbf{\varphi}} < 1$-basin with very high γ . With $(R = 2, r = 1)$, *i*) the classic player does not over rate the quantum one, *ii*) both players equalize at $\overline{p} = 1.5$ by $\gamma = \pi/4$, *iii*) the $\overline{\mathbf{p}}_{\mathbf{\varphi}} < 1$ region enlarges compared to the scenarios with greater R , as it commences at $\gamma = 3\pi/8$.

Examples of the dynamics and long-term patterns in the scenario of Fig. 6 with maximal entangling may be found in [2] . This article also consider the case of three-parameter quantum versus semi-quantum contests, semi-quantum referring to players that may not implement one of the *quantum* parameters, either α or β, but have access to the other one, β or α respectively (in both cases with the θ parameter operative). The effect of variable entanglement on quantum versus semi-quantum contests is shown in Figs. 7 and 8 . The changing predominance in Fig. 7 is highly surprising, and that of the (θ, α)-player in the highest range on γ fully unexpected. This is not the case in Fig. 8 , in which case

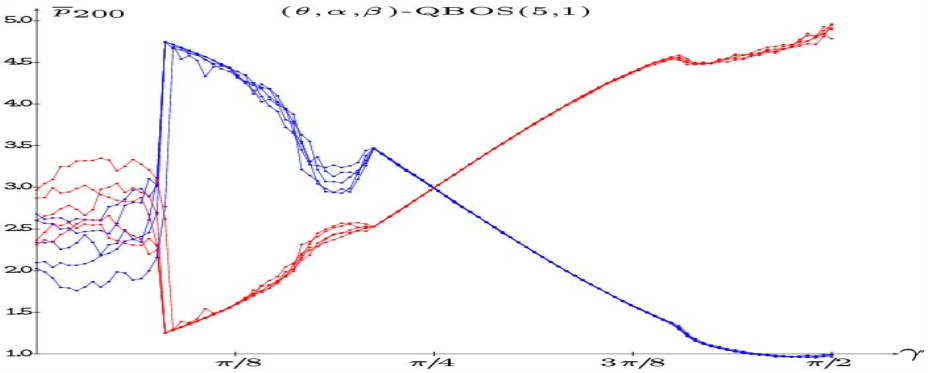

Fig. 6. Long-term mean payoffs in five simulations of an unfair three-parameter quantum (red) versus classic (blue) (5,1)-BOS CA with entanglement factor γ

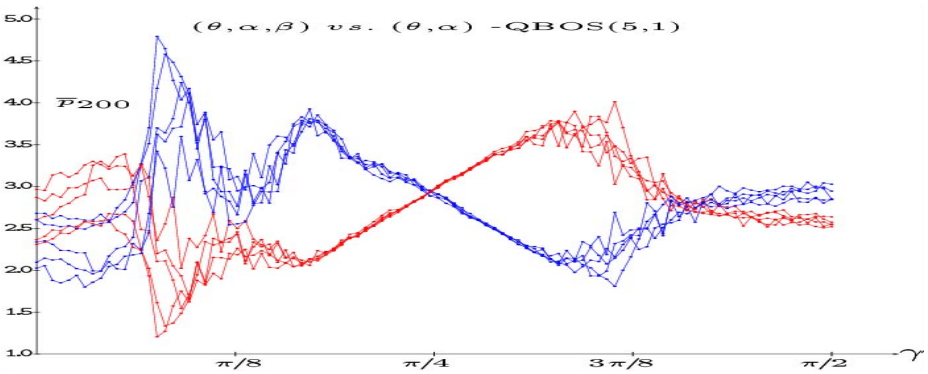

Fig. 7. Long-term mean payoffs in five simulations of a three-parameter quantum (red) versus (θ, α) semi-quantum (blue) (5,1)-BOS CA with entanglement factor γ

what is very notable is the wide range of γ values in which the (θ, β)-player over rates the quantum players, with no equalization at $\gamma = \pi/4$.

Again, it has been checked that the main features of the plots in the scenarios of Figs. 7 and 8 are preserved with the BOS parameters (4,1) and (6,1) . Nevertheless, the interval with *indefinite* plot appearance when γ is low varies at some extent : It is wider in the (4,1) model, and narrower with (6,1) BOS parameters. With $(R=2, r=1)$, the full quantum player over rates the (θ, α)-player from $\gamma = \pi/4$, whereas in the full quantum versus (θ, β) contest, the (θ, β)-player only slightly over-rates the full quantum player around the $[\pi/4, 3\pi/8]$ interval of γ .

Let us conclude this section by remarking that figures 7 and 8 make apparent that the role of the α and β parameters in the three-parameter model is fairly different.

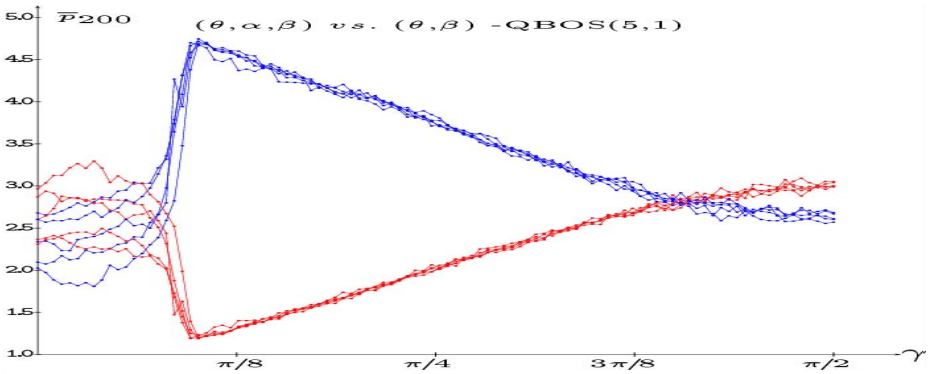

Fig. 8. Long-term mean payoffs in five simulations of a three-parameter quantum (red) versus (θ, β) semi-quantum (blue) (5,1)-BOS CA with entanglement factor γ

4 Conclusions and Future Work

The effect of variable entangling on the dynamics of a spatial quantum formulation of the iterated Battle of the Sexes (BOS) game is studied in this work. The game is played in the cellular automata (CA) manner, i.e., with local and synchronous interaction. The evolution is guided by the imitation of the best paid neighbour.

The effect of increasing the entangling factor (γ) differs notably when considering two or three parameter strategies. In the fair quantum versus quantum players scenario, *i*) with two-parameter strategies, the mean payoffs ($\overline{p}$) of the male player over rates those of the female players when γ is lower than 3/4 times its maximum value; beyond this value the female player over rates the male player, *ii*) with three-parameter strategies, the mean payoffs are not dramatically altered by the increase of γ , the main effect being a moderation in the variation of the $\overline{p}$ values .

In the unfair quantum versus classic scenario, *i*) with two-parameter strategies, the effect of increasing γ is somehow that expected : It boosts the quantum player to over rate the classic player, *ii*) with three-parameter strategies, if γ is over its middle value, the quantum player over rates the classic player, but in most of the parameter region below the γ-middle value, unexpectedly, the classic player over rates the quantum player. In unfair three-parameter quantum versus semi-quantum contests, highly surprising effects emerge, as the semi-quantum player over rates the full quantum player in wide γ regions.

The findings just reported apply precisely for the case of the $(R = 5, r = 1)$ BOS parameters. With more separated parameter values, such as $(R = 6, r = 1)$ the simulations that we have run confirm qualitatively the findings reported for (5,1), even in a more definite manner. With closer parameter values, we have tried (4,1), again the findings reported in this study qualitatively remain, albeit the details of the dynamics and the spatial structure of the parameter and

payoff patterns may vary notably in some cases. On the contrary, simulations run with close numerical values of the BOS parameters, such as (2,1), have proved to produce less definite dynamics, in particular when dealing with unfair contests. An analytical study of cellular automaton quantum games is due, albeit it appears to be very challenging.

Other quantization schemes [11,12] deserve to be studied in the spatial context. In particular, the scheme introduced by Marinatto and Weber [10,15], a model with no bias favouring to any of the players.

Further study is due on games with asynchronous and probabilistic updating, as well as on the effect of increasing degrees of spatial dismantling, and that of memory [4]. These are deviations from the canonical cellular automata paradigm which may lead to more realistic models.

Acknowledgment. This work was supported by the Spanish grant M2012-39101-C02-01. Part of the computations of this work were performed in EOLO and FISWULF, HPC machines of the International Campus of Excellence of Moncloa, funded by the Spanish Governement and Feder Funds.

References

1. Alonso-Sanz, R.: A quantum prisoner's dilemma cellular automaton. Proc. R. Soc. A 470, 20130793 (2014)
2. Alonso-Sanz, R.: On a three-parameter quantum battle of the sexes cellular automaton. Quantum Information Processing 12(5), 1835–1850 (2013)
3. Alonso-Sanz, R.: A quantum battle of the sexes cellular automaton. Proc. R. Soc. A 468, 3370–3383 (2012)
4. Alonso-Sanz, R.: Dynamical Systems with Memory. World Scientific Pub. (2011)
5. Benjamin, S.C., Hayden, P.M.: Comment on "Quantum games and quantum strategies". Physical Review Letters 87(6), 069801 (2001)
6. Du, J.F., Xu, X.D., Li, H., Zhou, X., Han, R., et al.: Entanglement playing a dominating role in quantum games. Physics Letters A 89(1-2), 9–15 (2001)
7. Du, J.F., Li, H., Xu, X.D., Zhou, X., Han, R.: Phase-transition-like behaviour of quantum games. J. Phys. A: Math. and Gen. 36(23), 6551–6562 (2003)
8. Eisert, J., Wilkens, M., Lewenstein, M.: Quantum games and quantum strategies. Physical Review Letters 83(15), 3077–3080 (1999)
9. Flitney, A.P., Abbott, D.: Advantage of a quantum player over a classical one in 2x2 quantum games. Proc. R. Soc. Lond. A 459(2038), 2463–2474 (2003)
10. Marinatto, L., Weber, T.: A quantum approach to static games of complete information. Physics Letters A 272, 291–303 (2000)
11. Nawaz, A., Toor, A.H.: Dilemma and quantum battle of sexes. J. Phys. A: Math. and General 37(15), 4437 (2004)
12. Nawaz, A., Toor, A.H.: Generalized quantization scheme for two-person non-zero sum games. J. Phys. A: Math. Gen. 37(47), 11457 (2004)
13. Nowak, N.M., May, R.M.: Evolutionary games and spatial chaos. Nature 359, 826–829 (1992)
14. Owen, G.: Game Theory. Academic Press (1995)
15. Situ, H.: A quantum approach to play asymmetric coordination games. Quantum Information Processing 13(3), 591–599 (2013)